Journal of Applied Polymer Science

Oligonucleotides-Decorated-Poly(*N*-vinyl pyrrolidone) Nanogels for Gene Delivery

Clelia Dispenza,[1,2] Giorgia Adamo,[3] Maria Antonietta Sabatino,[1] Natascia Grimaldi,[1] Donatella Bulone,[2] Maria Luisa Bondì,[4] Salvatrice Rigogliuso,[3] Giulio Ghersi[3]

[1]Dipartimento di Ingegneria Chimica, Gestionale, Informatica, Meccanica, Università degli Studi di Palermo, Viale delle Scienze, Edificio 6, 90128 Palermo, Italy

[2]CNR - Istituto di Biofisica (IBF) UOS Palermo, Via U. La Malfa, 153, 90146 Palermo, Italy

[3]Dipartimento di Scienze e Tecnologie Biologiche, Chimiche e Farmaceutiche (STEBICEF), Università degli Studi di Palermo, Viale delle Scienze, Edificio 16, 90128 Palermo, Italy

[4]CNR - Istituto per lo Studio dei Materiali Nanostrutturati (ISMN) UOS Palermo, via Ugo La Malfa, 153, 90146 Palermo, Italy

Correspondence to: C. Dispenza (E-mail: clelia.dispenza@unipa.it)

ABSTRACT: Pulsed electron-beam irradiation of a semi-dilute poly(*N*-vinyl pyrrolidone) (PVP) aqueous solution in the presence of acrylic acid has led to a carboxyl functionalized nanogel system. Nanoparticles hydrodynamic size and surface charge density, in water and as a function of pH, were investigated by dynamic light scattering and laser doppler velocimetry, respectively. Nanogels (NGs) were proved not to be cytotoxic at the cellular level. Indeed, they rapidly bypass the cellular membrane to accumulate in specific cell portions of the cytoplasm, in the perinuclear area. The availability of pendant carboxyl groups on the crosslinked PVP NGs core prompted us to attempt their decoration with a single strand oligonucleotide, which holds a terminal amino group. The recognition ability of the attached single helix of its complementary strand was investigated. © 2013 Wiley Periodicals, Inc. J. Appl. Polym. Sci. **2014**, *131*, 39774.

KEYWORDS: biomedical applications; gels; irradiation

Received 8 May 2013; accepted 18 July 2013

DOI: 10.1002/app.39774

INTRODUCTION

A big challenge in nanomedicine is the intracellular delivery of genetic material in conditions that can preserve its structure and ability to mediate biological processes. The most efficient gene vectors proposed up to date are viruses, because of their natural ability to transfect cells. However, viral vectors can produce adverse systemic immune responses, including patient fatalities. Moreover, without further genetic engineering, virus-targeting efficiency is limited to the specificity of the virus.[1,2] The incorporation or the chemical attachment of an oligonucleotide, siRNA, or DNA, on smart nanoparticles surface can offer the opportunity to efficiently transport genetic material within cells, limiting adverse side effects. Nanoparticles, because of their small size are able to penetrate within even small capillaries, to be taken up by cells. Receptor-mediated, site-specific localization can be also realized by decorating nanoparticles surface with targeting agents.[3] However, the development of therapeutic devices based on nanoparticles is still limited by the lack of synthetic strategies, which are simultaneously economically viable and able to grant a good degree of control over the device properties, especially when produced at a large scale. We have recently developed a single-step synthetic platform to generate either carboxyl or primary amino groups bearing poly(*N*-vinyl pyrrolidone) (PVP) nanogels.[4–7] The synthetic approach is based on high-energy irradiation of semi-dilute aqueous solutions of PVP in the presence of a functional group carrying acrylic monomer, namely acrylic acid. Polymer crosslinking, monomer grafting and sterilization are simultaneously achieved. The manufacturing process does not require long purification procedures, as it does when recourse to surfactants is made,[8] it can be easily scaled-up at industrial level with high throughputs and it ensures high control over materials properties, like particles size, surface charge densities, and degree of functionalization.[4,9] The produced nanogels, in virtue of the abundance of their reactive functional groups, can be decorated in mild reaction conditions with fluorescent probes and biomolecules.[4] Recently, several studies have demonstrated that nanogels can release active antisense oligonucleotides (ODN), which were shown to be able to produce some desired effects on gene expression in specific cell lines.[10] Furthermore, it has been

demonstrated that nanogels can transport ODN across cellular barriers, such as the blood–brain barrier (BBB) or monolayers of human intestine epithelial cells, thus ensuring ODN protection from enzymatic degradation.[11] Generally, nanogel-DNA complexes are prepared in physiological buffers through cooperative systems of salt bonds between the functional groups of a cationic polymer nanoparticle and the phosphate groups of DNA.[12] Recourse to surfactants is often made to improve colloidal stability of the complexes with adverse effects in efficiency, whereas in some cases DNA conformational changes have been observed.[13]

Herein, we describe the properties of a carboxyl functionalized PVP nanogel system, surface decorated with a single strand oligonucleotide. The bioconjugation reaction has been carried out using a terminal amino group present in the ODN to form an amide bond with one of the available carboxyl groups of the nanoparticles. The hydrodynamic size and surface charge density of the system in aqueous solutions and in a wide pH range (2.5–10) have been preliminarily investigated, as well as the absence of induced cytotoxicity and the ability of the nanoparticles to quickly bypass cell membranes. Subsequently, the pairing ability of the conjugated single strand oligonucleotide toward the complementary strand has been proved. In particular, purposely designed experiments where the nanoparticles decorated with a fluorescent variant of the ODN are annealed with the complementary strand, bearing a fluorescence quencher, were carried out. All the results gathered so far, strongly point out toward a possible application of these nanogels as nanocarriers for gene-delivery applications.

EXPERIMENTALS

Synthesis of Carboxyl-Functionalized Crosslinked-PVP Nanogels

An aqueous solutions of PVP K60 (Aldrich, $M_w = 4.1 \times 10^5$ g/mol, $R_h = 20 \pm 10$ nm from DLS measurements in water at 25°C)[14] at a concentration of 0.25 wt % in the presence of acrylic acid (AA, Aldrich), at a molar ratio between PVP repetitive unit and AA equal to 50, was prepared. The solution was carefully deoxygenated by gaseous nitrogen, bottled in hermetically closed glass vials and saturated by N_2O (99.99%) prior to irradiation. Electron beam irradiation was performed using the linear accelerator at the ICHTJ of Warsaw (Poland), Electronika 10/10. Irradiation was carried out at an average beam current of 0.45 mA, pulse length of 4.5 μs, and pulse repetition rate of 400 Hz.[4] Samples were horizontally placed in a box filled with ice and conveyed under the beam via a transporting belt at a speed of 0.3 m/min. An integrated dose of 40 kGy, within the sterilization dose range, was supplied with a single pass and at a dose-rate of 13 Gy per pulse.[15] After irradiation, samples were dialyzed (MWCO 100 kDa) against distilled water for 48 h to remove eventual unreacted monomer, oligomers, and low MW polymer and re-equilibrate pH.[4] The formulation had a pH of about 6.0 prior to irradiation, which turned to be 4.9 after irradiation and 5.8 after dialysis. The yield of recovered nanogels after dialysis was determined gravimetrically and resulted to be always above 95 wt %.[14] The system was coded P*(0.25)AA50.

Light Scattering and ζ Potential Measurements

The hydrodynamic diameters (D_h) of particles dispersed in water and in water solutions of different pH and same ionic strength were measured by dynamic light scattering (DLS).[4] Intensity autocorrelation function at the scattering angle of 90° and time autocorrelation function were measured by using a Brookhaven BI-9000 correlator and a 50 mW He−Ne laser (MellesGriot) tuned at $\lambda = 632.8$ nm. In consideration of the fact that samples showed a monomodal size distribution, DLS data were analyzed by the method of cumulants. Measurements were carried out on a minimum two samples from three independent runs, with excellent reproducibility.

Weight average molecular weights (Mw) were estimated from multiangle static light scattering measurements at 25°C ± 0.1°C in aqueous solution. The refractive index increment (*dn/dc*) of NGs system in aqueous solution was measured by using a Brookhaven Instruments differential refractometer at $\lambda = 620$ nm and resulted to be 0.1866 ± 0.002. Static light scattering data were analyzed according to the Zimm plot method.[16]

Surface charge densities of nanogels in water and in water solutions of different pH and same ionic strength was measured at 25°C using a ZetaSizer Nano ZS (Malvern Instruments, Malvern, UK) equipped with a He–Ne laser at a power of 4.0 mW. As for particle size distribution, also ζ potential measurements were carried out on minimum two samples from three independent runs, always showing consistent results.

Preparation of NGs Fluorescent Variant

The P*(0.25)AA50 NG system was labeled with a fluorescent probe, amino-fluorescein (AF), using an a standard protocol based on 1-ethyl-3-[3-dimethylaminopropyl]carbodiimide hydrochloride/N-hydroxysulfosuccinimide (EDC/sulfo-NHS, Aldrich).[17] The reaction was carried out at 25°C in 2-(N-morpholino)ethanesulfonic acid (MES, Aldrich) buffer at pH 5, in the excess of AF (molar ratio between AA in the irradiated solution and AF equal to 10), under continuous stirring. The probe-conjugated NG system was then purified through prolonged dialysis against water. Reaction and purification were both performed in the dark.

Conjugation degree was estimated by UV-Visible absorption measurements with Shimadzu 2401-PC spectrofluorimeter (scan speed 40 nm/min, integration time 2 sec, bandwidth 1 nm) at room temperature. Fluorescence spectra were acquired with a JASCO FP-6500 spectrofluorimeter, equipped with a Xenon lamp (150 W). Emission spectra, at the required excitation wavelength, were obtained with emission and excitation bandwidth of 1 and 3 nm, respectively. Samples were excited at the maximum absorption wavelength for AF (λ_{ex}=490 nm, λ_{em}=520 nm). The labeled sample is coded as P*(0.25)AA50-AF.

Cell Culture and Biological Studies

Human umbilical vein endothelial cells (ECV304) were grown and maintained using a suitable culture medium (MEM199, Euroclone, Celbar) supplemented with 10% fetal bovine serum (Euroclone, Celbar), 1% L-glutamine (Euroclone, Celbar), and 1% penicillin-streptomycin antibiotic solution (Euroclone, Celbar) at 37°C, in a humidified atmosphere of 5% CO_2.

Acridine-Orange Staining

ECV304 cells were plated on coverslip and grown in MEM199 complete medium for 24 h. Then, cells were incubated, respectively, at 60 and 250 μg/mL of P*(0.25)AA50 nanogels for 24 h. After the incubation period, the medium was removed and cells were washed with PBS; subsequently, cells were stained with Acridine Orange PBS solution (Sigma) at 100 µg/mL for 10 min at room temperature and quickly examined by fluorescence microscopy (Leica, DFC450C). Acridine Orange is a cell-permeating nucleic acid binding dye that emits green fluorescence when bound to double-strand DNA and red fluorescence when bound to single-strand DNA or RNA. This staining discriminates between alive (green nuclei) to damaged (red nuclei) cells. As a positive control, cells were treated with Doxorubicin (DXR, Ebewe Pharma) at 5 µ*M* for 24 h.

Apoptosis Evaluation by Enzymatic Assay

ECV304 were seeded at a density of 5×10^5 cells/well in a six-well plate and cultured for 24 h in MEM199 complete medium; afterwards, cells were incubated at 250 μg/mL of P*(0.25)AA 50 for 24 h. Cells were enzymatically detached using Trypsin-EDTA 1X (Sigma) solution and centrifuged at 1000 rpm for 5 min. Pelleted cells were lysed in 70 μL of 1% Triton X 100 solution in PBS, incubated 10 min at room temperature and successively centrifuged at 10.000 rpm for 10 min. The amount of protein extract in the supernatant medium was quantified using Bradford micro-assay method (Bio-Rad, Segrate, Milan, Italy). A standard curve built with a known amount of BSA (Sigma-Aldrich) was used as a reference. ECV304 cells extracts (20 μg), obtained as previously described, were used to detect the presence of activated Caspases 3/7/8, that is a typical apoptosis marker, using Asp.Ac-Glu-Val-Asp-MCA peptide (Pepta Nova, 380 Peptide Institute).[18,19] This specific substrate for Caspases has a fluorophorein its cleavage site, which emits fluorescence when cleaved by these enzymes, suggesting that mechanisms of cell death have been activated. The degree of Caspase activation was quantified by spectrofluorimetric readings using Spectra Max Gemini EM-500 (Molecular Devices) and elaborated by SoftMax Pro 5.2 software.

Untreated ECV304 cells were used as negative control and cell treated with DXR at 5 μ*M* for 24 h, as positive control.

Cell Viability Assay

Cellular viability was determined using the MTT assay (Sigma). Cells were seeded in a 96-well plates at a density of 1×10^4 cell/well. After 24 h from seeding, cells were incubated for a further 24 h at different concentrations (30, 60, 120 μg/mL) of P*(0.25)AA50 particle suspension. Nontreated cells were used as negative control and treated cells with of DXR at 5 μ*M* for 24 h were used as positive control. Cell viability was evaluated using MTT reagent. MTT (0.25 mg/mL) solution was added to each well; the plates were incubated for 2 h at 37°C. The insoluble formazan crystals, produced in the mitochondrial compartment of viable cells, were dissolved using dimethyl sulfoxide (DMSO, 100 μL/well). The purple solution, obtained from enzymatic reaction with the mitochondrial dehydrogenase of alive cells, was read at a wavelength of 490 nm using a DU-730 Life Science spectrophotometer (Beckman Coulter). The percentage of cell viability was calculated as ratio between each sample with respect to the negative control (100% of cell viability).

Cellular Internalization Studies by Confocal Analysis

ECV 304 cells were grown at a density of 5×10^3 cells/well in 12-well plates containing sterile coverslips in complete medium MEM199 for 24 h. Cells were incubated at 120 μg/mL of P*(0.25)AA50-AF. At different incubation times, and in particular 1, 3, 6, and 24 h, cells were quickly washed with PBS to remove nanoparticles that were loosely bound to the cellular membrane, fixed with 3.7% of formaldehyde for 15 min, and washed again twice with PBS. Afterward, cells were stained for 1 min at room temperature with Ethidium Bromide (EtBr 1:1000). Nanoparticles localization inside cells was monitored by confocal microscopy analysis (Olympus 1×70 with 419 Melles Griot laser system).

Functionalization of Nanogels with ODN

Modified ODN used were FAM-FW-N (FAM-5'-AAA ACT GCA GCC AAT GTA ATC GAA-3'-NH2), REV-BHQ1 (5'-TTC GAT TAC ATT GGC TGC AGT TTT-3'-BHQ1), G1-REV-N (5'-TTC GAT TAC ATT GGC TGC AGT TTT-3') (Eurofins). P*(0.25)AA50-FAM-FW-N conjugates were prepared using an EDC/SulfoNHS coupling solution. FAM-FW-N has been directly attached to the carboxyl groups of nanogels through the C3-amine modified link at 3′ end (see Scheme 1A)

Firstly, 200 µL of P*(0.25)AA50 were incubated with EDC/NHS solution for 30 min at 37°C, while gentle stirring was provided; then, 1.0 µL of FAM-FW-N (2.5×10^{-2} µmol) was added and incubated for 3 h at 37°C, while stirring. The same solution, without FAM-FW-N, was also prepared and used as control. Both oligonucleotide-conjugated systems (P*(0.25)AA50-FAM-FW-N) and the relative control were thoroughly dialyzed (72 h) against milli-Q water using membranes with MWCO 14 kDa, to remove the nonconjugated oligonucleotide. In order to confirm the occurrence of conjugation and quantify the amount of oligonucleotide effectively conjugated, the fluorescence emitted by the FAM fluorophore (excitation 495 nm, emission 520 nm) present on the 5′end of the oligonucleotide FAM-FW-N was estimated using GloMax® Multi System (Promega). A calibration curve was made using solutions with increasing concentrations of FAM-FW-N.

Annealing and Digestion Test using Oligonucleotide-Conjugated Nanogels

In order to verify the accessibility by the complementary semi-helix to the oligonucleotide conjugated to the nanoparticles, an annealing test with was performed (see Scheme 1B).

The annealing reaction was carried out using a thermocycler (Perkin Elmer, GeneAmp PCR system), in which two thermal cycles were carried for the P*(0.25)AA50-FAM-FW-N system in the presence of REV-BHQ1, 50 m*M* NaCl, TE buffer 1X (10 m*M* Tris-Cl pH 7.5, 1 m*M* EDTA), passing through the specific annealing temperature of the two sequences.

After the annealing step, samples were washed many times with an equal volume of milli-Q water to remove the not annealed REV-BHQ1, using 100 kDa spin-dryer filters (Amicon) at 300 rpm. As negative control, the same reaction was carried out

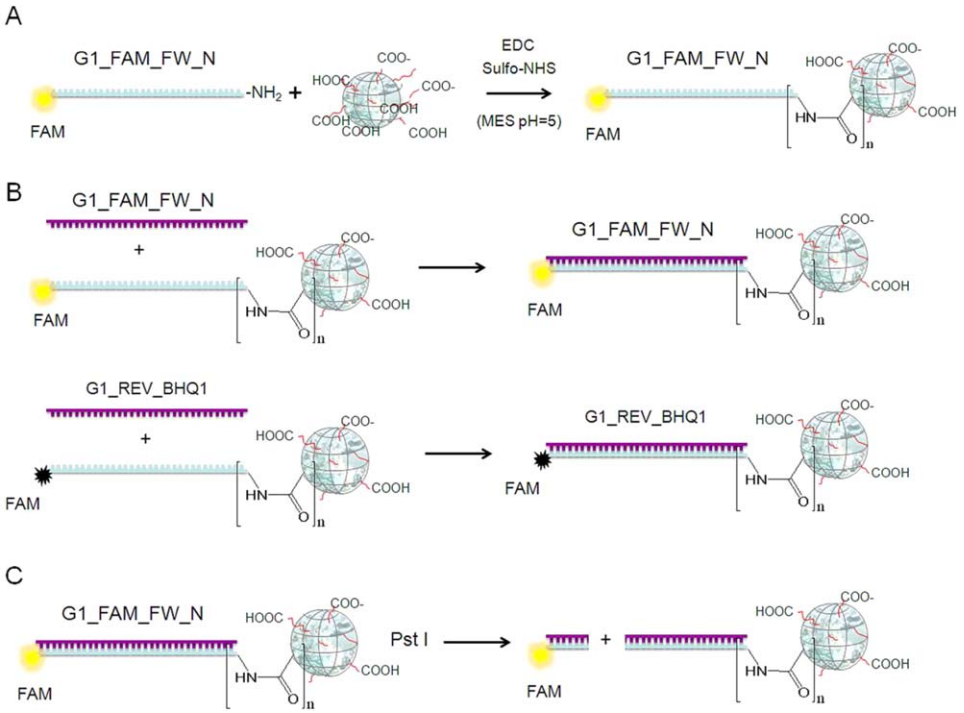

Scheme 1. (A) Conjugation of P*(0.25)AA50 nanogels with a single strand oligonucleotide (FAM-FW-N) bearing a fluorescent label (FAM). (B) Annealing reaction of P*(0.25)AA50-FAM-FW-N with the complementary semi-helix with (REV-BHQ1) and without (G1-REV-N) a fluorescence quencher. (C) Digestion of FAM-FW-N conjugated P*(0.25)AA50 nanogels with the sequence-specific cutting enzyme Pst I. [Color figure can be viewed in the online issue, which is available at wileyonlinelibrary.com.]

using G1-REV-N, the complementary oligonucleotide lacking of the quencher. Finally, the FAM-fluorescence present in both samples was detected by GloMax® Multi System 3.

As the oligonucleotide sequences brought are cognition site for a specific restriction enzyme, the Pst I endonuclease, the double-strand DNA-nanoparticles, obtained after the annealing were incubated with Pst I (75 μ/mL; BioLabs) in their appropriate buffer, at 37°C for 2 h (see Scheme 1C). After the digestion step, the samples were washed 20 times with an equal volume of milli-Q water, using 100 kDa spin-dryer filters at 300 rpm, to remove the DNA fragments cleaved by Pst I. These washings were lyophilized and suspended again in 100 μL of milli-Q water. Then, the FAM-fluorescence present in the wash was detected by GloMax® Multi System 3.

RESULTS AND DISCUSSION

Nanogels Physicochemical and Molecular Properties

An easy, robust, and scalable at industrial level synthetic approach is at the basis of the development of therapeutic devices based on radiation-engineered carboxyl functionalized PVP nanogels.[4,14] Here we describe the main physicochemical and molecular properties of a selected acrylic acid-grafted-PVP system used for conjugation with ODN. In particular, in Table I mean hydrodynamic diameter (D_h), ζ-potential in water (pH = 6), and weight average molecular weight (MW) values for the P*(0.25)AA50 NGs system are shown. The average hydrodynamic diameter of the NGs is 26 ± 9 nm. The ζ-potential plot shows a markedly anionic behavior of the nanogels dispersed in water, with a single narrow peak. The small particle size and the anionic character grant the colloidal stability of the system in water solution. Indeed, we do not have observed precipitation even after prolonged storage. Chemical composition of P*(0.25)AA50 NGs was also characterized through spectroscopic analysis and closely resembles that of PVP.[6]

Hydrodynamic size and surface charge density were also measured in water solutions at different pHs (2.5–10) and controlled ionic strength (1 m*M*). Data are displayed in Figure 1. Particles size distributions are monomodal for all the pHs and the hydrodynamic size of NGs is almost invariant with pH when above 5. At pH below the pKa of AA (pKa=4.75), a great proportion of carboxyl groups present on nanogels becomes protonated and the corresponding ζ-potential value approaches 0 mV. The fading of the electrostatic charge repulsion as well as the related increase of hydrophobicity lead to NGs aggregation and their precipitation upon storage. At pH above the pKa of AA, ζ-potentials are negative and their absolute values increase with pH because of the progressive dissociation of carboxyl groups. As the protonation state of carboxyl groups does not significantly affect the hydrodynamic size of the nanogels, but only

Table I. Average Hydrodynamic Diameter (D_h), ζ-Potential in Water (pH 6) and Weight Average Molecular Weight of the Polymer (MW) for P*(0.25)AA50 NGs

Sample	D_h (nm)	ζ-potential (mV)	Zeta dev. (mV)	MW (MDa)
P*(0.25)AA50	26 ± 9	−40	9.26	1.02

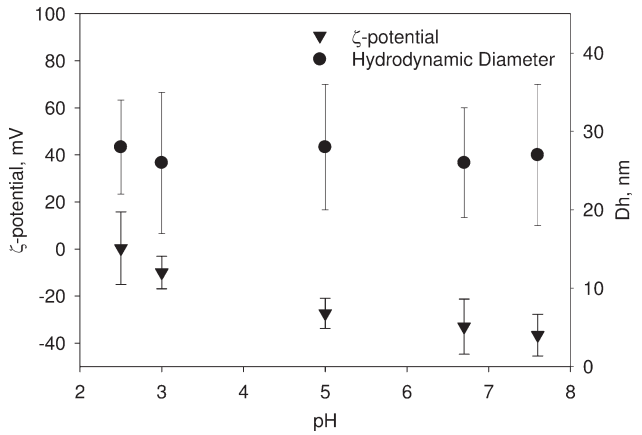

Figure 1. Average hydrodynamic diameters and ζ-potential values of NG dispersions in water at the variance of pH and constant ionic strength (1 m*M*). Error bars represent the width of particles size or surface charge density distributions.

their surface charge density, we expect these groups to be mainly present as grafted arms on the crosslinked PVP cores.

In order to verify if nanogels are able to bypass the cell plasma-membrane and localize in specific cell districts, localization studies in cell cultures were performed. For the purpose, P*(0.25)AA50 system was labeled with a green emissive fluorescent probe. The conjugation degree, reported as molar ratio between ligand and nanoparticle, estimated through UV-Vis absorption measurements, is equal to 5. The emissivity of probe labeled NGs was also tested through UV-Vis emission spectroscopy. Figure 2 shows the comparison between the non-emissive bare system and its fluorescent variant.

Biological Evaluations

Nanogels biocompatibility was tested by *in vitro* assays. To verify the absence of apoptotic events, a morphological evaluation by fluorescence microscopy analyses was performed on ECV304 cells incubated with different concentration of NGs and stained with an Acridine Orange solution (Figure 3A). As it can be observed in Figure 3A (panel c-d), cells incubated respectively at 60 and 250 μg/mL of P*(0.25)AA50 do not show the classical morphological changes associated with apoptotic events. Indeed, cells show mainly uniform bright green nuclei with organized structures, similarly to the negative control (panel a). Conversely, damaged DNA is evident in cells treated with DXR (panel b), which are characterized by red nuclei with condensed or fragmented chromatin.

In order to further support this evidence, an enzymatic assay was carried out using the Ac.Asp-Glu-Val-Asp-MCA substrate, a selective fluorogenic peptide for identification and quantification of Caspases 3,7,8 activity. The fluorogenic MCA residue, released by activated Caspase cleavage, was quantified by spectrofluorimeter readings. ECV304 cells, treated or not (negative control) at 250 μg/mL of P*(0.25)AA50 nanoparticles for 24 h were compared with the ones treated with DXR (positive control). At different incubation times with the Caspase substrate,

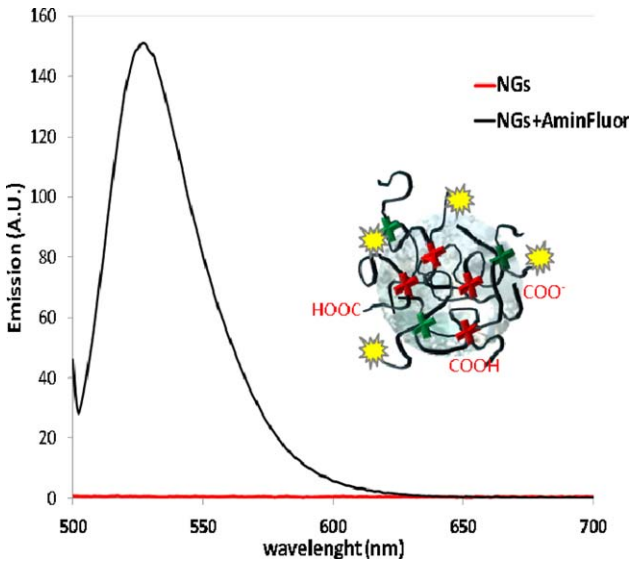

Figure 2. UV-Vis emission spectra of P*(0.25)AA50 and its fluorescent variant. [Color figure can be viewed in the online issue, which is available at wileyonlinelibrary.com.]

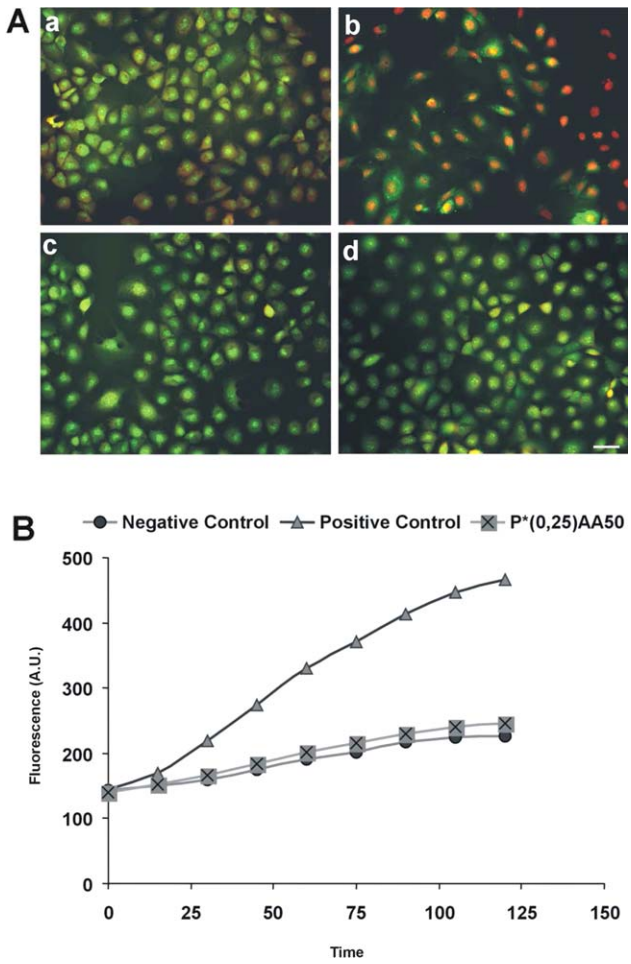

Figure 3. A: Apoptotic evaluation by AO on ECV304 cells: (a) untreated; (b) in the presence of DXR [5 μ*M*]; (c) incubated with nanogelsat 60 μg/mL; and (d) at 250 μg/mL for 24 h. Magnification 20×. Bar = 100 μm. B: Enzymatic Caspase 3 substrate activation. [Color figure can be viewed in the online issue, which is available at wileyonlinelibrary.com.]

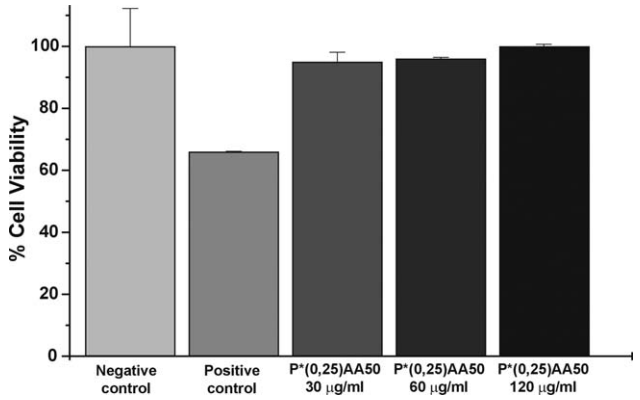

Figure 4. Cytotoxicity evaluations by MTT assay. Percentage of cell viability is expressed with reference to the untreated cells.

ECV304 cells' extracts were analyzed to determine the amount of fluorescence of each sample. As shown in Figure 3B, NGs-treated cells did not show any activation of Caspases, while time-dependent fluorochrome release was observed for the DXR-treated cells (positive control). These results confirm the absence of programmed cell death induced by the presence of P*(0.25)AA50 nanogels.

The absence of cytotoxicity of P*(0.25)AA50 nanogels was also evaluated by the MTT viability assay. Figure 4 shows the relative viability of ECV304 cells after 24 h of incubation in the presence of different amount of nanogels. It is evident that the viability of the cells in the presence of nanogels is similar to that of the negative control (untreated cells), differently from the DXR-treated cells (positive control), which show a mortality increase. As a result of both the morphological evaluation and the MTT assay, we can conclude that the nanogels show very good biocompatibility.

Nanogels Localization in Cell Culture

In order to verify if the nanogels are able to bypass the cell plasma-membrane and to localize in specific cell districts, localization studies in cell cultures were performed. ECV304 cells were treated for different incubation times with the aminofluorescein labeled variant of the NGs; their movement through cell membrane and localization inside cells was followed by confocal microscopy analysis. As shown in Figure 5, the amount of NGs inside the cells slowly increases, after 1 h (A) and further after 3 h (B) of incubation to reach its maximum concentration in the cytoplasm compartments, and particularly in the perinuclear area, after 6 h (C). After 24 h, (D) evidence of cytoplasmic

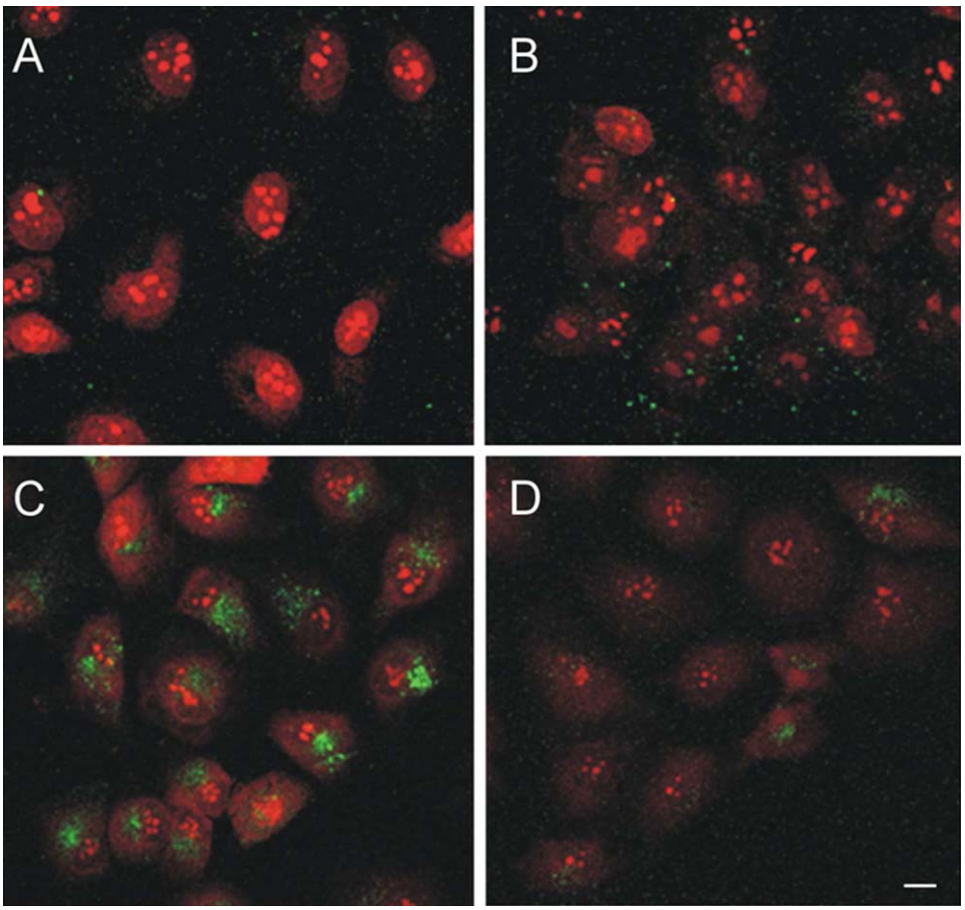

Figure 5. Localization study by confocal microscopy analysis of aminofluorescein conjugated nanogels incubated on ECV304 cells for: (A) 1 h; (B) 3 h; (C) 6 h; and (D) 24 h. Cells were stained with EtBr (Red). Magnification 40×. Bar = 10 μm. [Color figure can be viewed in the online issue, which is available at wileyonlinelibrary.com.]

localization of NGs is still present, although at lower concentration. It is interesting to observe that the pattern of the nanogels localization in cell culture is similar to that observed for the amino-functionalized crosslinked PVP nanogels obtained by either radiation-processing[4] or by a inverse microemulsion chemical polymerization.[8] A similar perinuclear localization has been also documented for a number of different nanoparticulate carriers and bio-hybrid conjugates, such as Au NPs conjugated both with antisense ODN and/or synthetic peptides,[20] DNA-containing gelatin and PEGylated gelatin NPs[21] or polyethylenimine/DNA nanocomplexes.[22] While the specific mechanism of the internalization process of our NGs is currently under investigation, some general hypotheses can be proposed on the account of the analogies with other systems described in the literature. The endocytic pathway is often proposed as the major cellular uptake mechanism of any biological agent or biomolecular therapeutics-carrying nanoparticle. Particles or biological entities entering the cells through the endocytic pathway become entrapped in the endosomes, where they experience a pH change from ~7 to ~5, and eventually end up in the lysosomes, where active enzymatic degradation processes take place. In order to protect the nanocarrier contents from degradation and ensure their cytosolic delivery, strategies for facilitating the "endosomal escape" of the loaded carrier have to be set in place. Several approaches have been attempted for the purpose.[23] For pH-responsive synthetic polymers either proton-sponge effects or membrane-destabilizing activities have been often proposed [Ref. [23] and references herein]. In particular, the pH-dependent, membrane-destabilizing activity of poly(alkylacrylic acid) polymers has been described by Hoffman and coworkers.[24,25] Protonation of the carboxyl acid groups placed at the end of relatively short (C2-C4) lateral alkyl chains in the polymer reversibly transform the hydrophilic "stealth-like" polymers at physiologic pH into hydrophobic membrane-destabilizing nanoparticles. With reference to the carboxyl functionalized PVP nanogels here described, we already demonstrated that alongside intra- and inter-molecular crosslinking of poly(N-vinyl pyrrolidone) also significant degradation reactions can occur with possible pyrrolidone ring opening and subsequent formation of butyric acid pendant groups.[7] These groups may be responsible for the hydrophilic to hydrophobic conversion of nanogels, which is also at the basis of the observed colloidal destabilization of dispersions at pH < 5.

Nanogels Functionalization with Modified ODN

The FAM-FW-N oligonucleotide was built with a C3-aminolink at the 3′-end, capable of reacting with the carboxyl groups present on nanogels, and with FAM fluorochrome at the 5′-end, in order to make the oligonucleotide fluorescent. The amount of oligonucleotide linked to nanoparticles was estimated by fluorimetric analysis. As nanoparticles present a slight self-fluorescence in correspondence of FAM emission peak (520 nm), this contribution was subtracted to the emission intensity of oligonucleotide conjugated-nanogels. The absolute emission intensity of nanogels and oligonucleotide conjugated-nanogels are shown in Figure 6. In order to exclude a non-specific attachment of the ODN to the nanoparticle and to verify that it maintains its ability to form a double-strand DNA, an annealing test was performed. For the annealing test, two different types of complementary sequences were used, with and without a FAM-black hole quencher. As shown in Figure 6, after two cycles at the annealing temperature, the FAM fluorescence is quenched (20 times lower) when NGs are annealed in the presence of REV-BHQ1. Conversely, when the annealing test was performed with the complementary sequence without the quencher, the FAM fluorescence is not attenuated. This experimental evidence shows that even if the FAM-FW-N sequence is linked to the nanogels, it takes the correct folding reacting with the correct complementary sequence. To further support this evidence, Pst I restriction enzyme digestion was performed. As a consequence of the enzymatic cut, the double helix of DNA formed upon annealing looses the 5′ end that carries the FAM fluorochrome. The digestion products were separated from the NGs and their fluorescence was measured. After the digestion nanogels conjugated and annealed with the complementary sequences (with or without the quencher) show only their initial auto-fluorescence values (data not shown). This result corroborates the previous one, as the sequence-specific cutting operated by the enzyme Pst I works only if the base pairing is specific, i.e. without DNA mismatching.

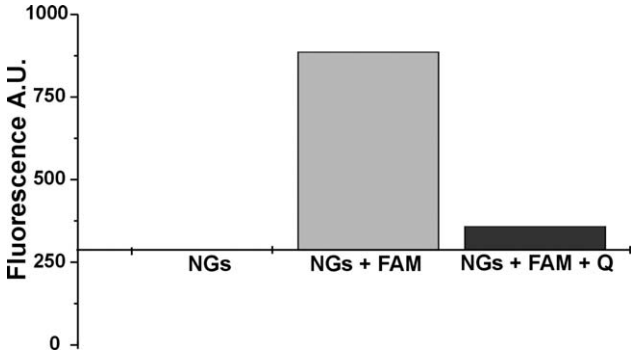

Figure 6. Fluorescence intensity of bare nanogels (NGs), FAM-FW-N conjugated nanogels (NGs + FAM) and FAM-FW-N conjugated nanogels after annealing with REV-BHQ1 (NGs + FAM + Q).

CONCLUSIONS

Nanogels, formed by radiation-induced crosslinking of PVP and simultaneous grafting of acrylic acid, were obtained quantitatively and reproducibly by electron-beam irradiation of semi-dilute aqueous solutions of the polymer. At the selected irradiation dose of 40 kGy, system sterility is also achieved. As a result, nanogels with a crosslinked PVP core and AA groups bearing arms form. A good control of hydrodynamic size of nanogels at the nanoscale is achieved. Furthermore, nanogels show a net negative surface charge density at physiological pHs, which collaborate to their colloidal stability. The availability of carboxyl groups prompted us to attempt the attachment of a single strand oligonucleotide by its terminal amino group in a way that preserved its pairing ability with the complementary strand. Absence of induced cytotoxicity by these nanoparticles and their ability to bypass cell membranes, to then localize in the perinuclear area of the cytoplasm, encourage a further development of these nanocarriers as intracellular delivery devices of genetic material for therapeutic purposes.

ACKNOWLEDGMENTS

This research was supported by a grant from the Italian Ministry of University and Scientific Research (PRIN 2010-2011 NANOMED). We acknowledge the assistance of the Centre for Radiation Research and Technology, Institute of Nuclear Chemistry and Technology, Warsaw, Poland for e-beam irradiation.

REFERENCES

1. Mintzer, M. A.; Simanek, E. E. *Chem. Rev.* **2009**, *109*, 259.
2. Morille, M.; Passirani, C.; Vonarbourg, A.; Clavreul, A.; Benoit, J. -P. *Biomaterials* **2008**, *29*, 3477.
3. Byrne, J. D.; Betancourt, T.; Brannon-Peppas, L. *Adv. Drug Deliver. Rev.* **2008**, *60*, 1615.
4. Dispenza, C.; Sabatino, M. A.; Grimaldi, N.; Bulone, D.; Bondì, M. L.; Casaletto, M. P.; Rigogliuso, S.; Adamo, G.; Ghersi, G. *Biomacromolecules* **2012**, *13*, 1805.
5. Dispenza, C., Sabatino, M. A., Grimaldi, N., Spadaro, G., Bulone, D., Bondì, M. L., Adamo, G., Rigogliuso, S. *Chem. Eng. Trans.* **2012**, *27*, 229.
6. Grimaldi, N.; Sabatino, M. A.; Przybytniak, G.; Kaluska, I.; Bondì, M. L.; Bulone, D.; Alessi, S.; Spadaro, G.; Dispenza, C. *Rad. Phys. Chem.* doi:10.1016/j.radphyschem.**2013**.*04*.012.
7. Sabatino, M. A.; Bulone, D.; Veres, M.; Spinella, A.; Spadaro, G.; Dispenza, C. *Polymer* **2013**, *54*, 54.
8. Dispenza, C.; Grimaldi, N.; Sabatino, M. A.; Bulone, D.; Bondi, M. L.; Rigogliuso, S.; Ghersi, G. *React. Funct. Polym.* **2013**, *73*,1103.
9. Ulanski, P.; Rosiak, J.M. In: Encyclopedia of Nanoscience and Nanotechnology, Nalwa, H. S., Ed.; American Scientific Publishers: Valencia, CA, USA, **2004**; p 1.
10. Vinogradov, S. V.; Batrakova E. V.; Kabanov A. V. *Colloid Surf. B* **1999**, *16*, 291.
11. Vinogradov, S. V.; Batrakova, E. V.; Kabanov, A. V. *Bioconjug. Chem.* **2004**, *15*, 50.
12. Lemieux, P.; Vinogradov S. V.; Gebhart C. L.; Guérin, N.; Paradis, G.; Nguyen H. K.; Ochietti, B.; Suzdaltseva Y. G.; Bartakova E. V.; Bronich T. K.; St-Pierre, Y.; Alakhov, V. Y.; Kabanov A. V. *J Drug Target.* **2000**, *8*, 91.
13. Mitra, A.; Imae, T. *Biomacromolecules* **2004**, *5*,69
14. Dispenza, C.; Grimaldi, N.; Sabatino, M. A.; Todaro, S.; Bulone, D.; Giacomazza, D.; Przybytniak, G.; Alessi, S.; Spadaro, G. *Radiat. Phys. Chem.* **2012**, *81*, 1349.
15. Lambert, B. J.; Hansen, J. M. *Radiat. Phys. Chem.* **1998**, *52*, 11.
16. Stepanek, P. Data analysis in dynamic light scattering. In Dynamic Light Scattering, Brown, W., Ed.; Oxford University Press: Oxford, **1993**; p 177.
17. Hermanson, G. T. Bioconjugate Techniques, 2nd ed.; Academic Press: New York, **2008**.
18. Nicholson, D. W.; Ali, A.; Thornberry, N. A.; Vaillancourt, J. P.; Ding, C. K.; Gallant, M.; Gareau, Y.; Griffin, P. R.; Labelle, M.; Lazebnik, Y. A. *Nature* **1995**, *6*, 37.
19. Thornberry, N. A.; Rano, T. A.; Peterson, E. P.; Rasper, D. M.; Timkey, T.; Garcia-Calvo, M.; Nordstrom, P. A.; Roy, S.; Vaillancourt, J. P.; Chapman, K. T.; Nicholson, D. W. J. *Biol. Chem.* **1997**, *18*, 17907.
20. Patel, P. C.; Giljohann, D. A.; Seferos, D. S.; Mirkin, C. A. *Proc. Natl. Acad. Sci. USA* **2008**, *105*,17222.
21. Kaul, G.; Amiji, M. *J. Pharma. Sci.* **2005**, *94*, 184.
22. Suh, J.; Wirtz, D.; Hanes, J. *Proc. Natl. Acad. Sci. USA* **2003**, *100*, 3878.
23. Varkouhi, A. K.; Scholte, M.; Storm, G.; Haisma H. J. *J. Control. Release* **2011**, *151*, 220.
24. Cheung, C. Y.; Murthy, N.; Stayton, P. S.; Hoffman, A. S. *Bioconjug. Chem.* **2001**, *12*, 906.
25. Convertine, A. J.; Benoit, D. S. W.; Duvall, C. L.; Hoffman, A. S.; Stayton, P. S. *J. Control. Release* **2009**, *113*, 221.